IMECE2015-50930

THERMO-STRUCTURAL DESIGN OF THE HEXAFLY-INT EXPERIMENTAL FLIGHT TEST VEHICLE (EFTV)

Roberto Scigliano
Italian Aerospace Research Centre (CIRA)
Capua, Italy

Valerio Carandente
Italian Aerospace Research Centre (CIRA)
Capua, Italy

Nunzia Favaloro
Italian Aerospace Research
Centre (CIRA)
Capua, Italy

Salvatore Cardone
Tecnosistem Engineering &
Technology
Naples, Italy

Johan Steelant
European Space Agency (ESA)
Noordwijk, Netherlands

ABSTRACT

The Hexafly-INT project intends to test in free-flight conditions an innovative gliding vehicle with several breakthrough technologies on-board. This approach will create the basis to gradually increase the readiness level of a consistent number of technologies suitable for high-speed flying systems.
This paper presents a Finite Element thermal analysis of the Experimental Flight Test Vehicle, combining information coming from the flight trajectory, the structural layout, the vehicle aerothermodynamics and the thermal behavior of the preliminarily selected materials in high temperature conditions. Numerical results show the thermal performances of the selected high temperature resistant materials in moderate enthalpy flow conditions and provide fundamental information on the thermal loads to be considered for structural analyses.

1. INTRODUCTION

Over the last years, innovative concepts of civil high-speed transportation vehicles and the development of related technologies were proposed in European Commission co-funded projects like ATLLAS, LAPCAT and HEXAFLY [1,2,3]. These vehicles have a strong potential to increase the cruise range efficiency at high Mach numbers, thanks to efficient propulsion units combined with high-lifting vehicle concepts [4,5].

Nonetheless, performing a flight test will be the only and ultimate proof to demonstrate the technical feasibility of these new promising concepts and technologies and would result into a major breakthrough in high-speed flight. At present, the expected performances are usually demonstrated by numerical simulations and only partly by experimental tests. As high-speed wind tunnels are intrinsically limited in size, it is nearly impossible to completely fit even modest vehicle planform into a tunnel. Though numerical simulations are less restrictive in geometrical size, they struggle however with accumulated uncertainties in their modelling, making predictions doubtful without inflight validation. As a consequence, the obtained technology developments are now limited to a Technology Readiness Level (TRL) equal to 4 (components validated in laboratory).

The HEXAFLY-INT project aims at the free flight testing of an innovative high-speed vehicle with several breakthrough technologies on board [6,7]. This approach will create the basis to gradually increase the TRL.

The vehicle design, manufacturing, assembly and verification will be the main driver and challenge in this project, in combination with a mission tuned sounding rocket. The prime objectives of this free-flying high-speed cruise vehicle shall aim at [4]:

- a conceptual design demonstrating a high aerodynamic efficiency at cruise conditions with a high volumetric efficiency;
- a positive aerodynamic balance at a controlled cruise Mach numbers from 7 to 8;
- a good gliding performance from Mach 7 to 2;
- an optimal use of advanced high-temperature resistant materials and/or structures.

The main flight sequence profile and mission events are shown in Figure 1 and listed in Table 1 [5,8,9]. In particular, from Figure 1 and Table 1 it is evident that the separation between the launcher and the whole vehicle, consisting of the Experimental Flight Test Vehicle (EFTV) and the Experimental Support Module (ESM), occurs around the apogee of the sounding rocket parabolic trajectory. Then, in the first part of the descent, the vehicle attitude is controlled by the Cold Gas System (CGS) included in the ESM. When the dynamic pressure along the flight path is large enough to guarantee the aerodynamic manoeuvrability of the EFTV, the ESM is released. Finally, after a pull out manoeuvre, the EFTV starts its aerodynamically controlled cruise flight. The analysed EFTV and ESM configurations are shown in Figure 2 [8].

In the present work the methodology and the implementation of tools for thermal analysis of the EFTV, during a preliminarily considered test window, is presented [9]. Thermal analyses are performed on the basis of the trajectory provided by Gas Dynamics Limited (GDL) and of the structural layout developed by Tecnosistem Engineering & Technology (TET).

In particular, the calculations show a first feasibility analysis for the preliminarily selected materials.

2. FLIGHT TRAJECTORY

Flight mechanic analyses developed so far refer to different altitudes of the ESM release from the EFTV. For instance, Figure 3 shows the trajectory obtained for an EFTV mass of 350 kg assuming the ESM ejection at 50 km altitude. In particular, Figure 3 provides the time histories of altitude and velocity during descent, starting from the ESM release. This preliminary trajectory results in the most conservative scenario in terms of aero-thermal and mechanical loads available so far. The stagnation point convective heat transfer coefficient profile of the EFTV, provided in non-dimensional form as input to the thermal analysis hereinafter discussed, is shown in Figure 4. It was derived from the corresponding convective heat flux, estimated by means of the Tauber's [10] relationship throughout the descent flight shown in Figure 3. The EFTV nose leading edge radius is 2 mm and the aerothermal loading conditions refer to radiatively cooled walls with a surface emissivity of 0.4.
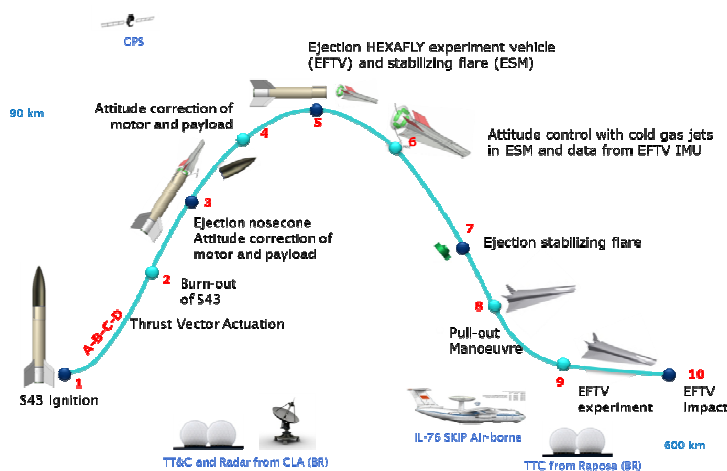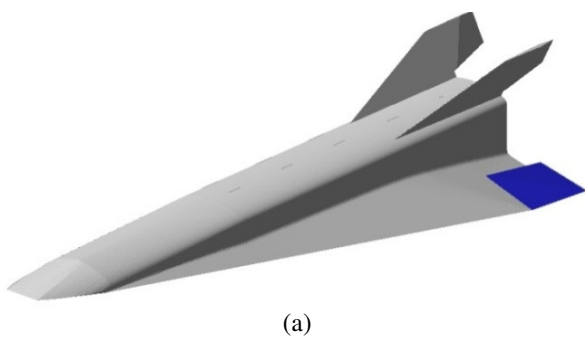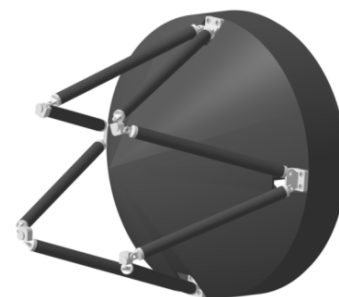

Figure 1. Flight sequence profile [5]

#	Flight Event
1-2	Propelled ascent
2	Motor burnout
3	Nose-cone ejection
4	L/V alignment
5	ESM/EFTV release
6	Attitude control by CGS in the ESM
7	Ejection of ESM
8	Pull-out manoeuvre
9	Controlled flight
10	Impact

Table 1. Flight sequence events [5]

(a)   (b)

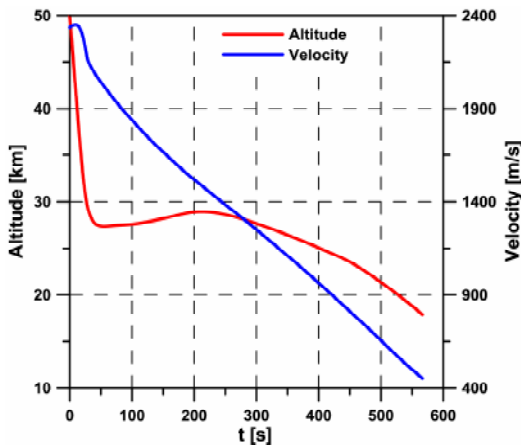*Figure 2. EFTV (a) and ESM (b) configurations analyzed [8]*

2

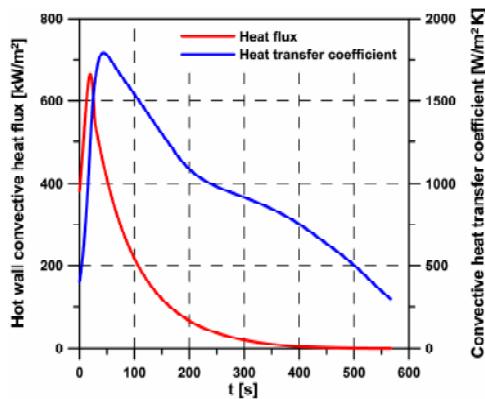*Figure 3. Altitude and velocity profiles for the considered flight path of EFTV vehicle*

Figure 4. Stagnation point convective heat flux estimated by means of Tauber's formula (radiation equilibrium condition) and corresponding convective heat transfer coefficient along the considered flight path

3. EFTV CANDIDATE MATERIALS

Different classes of materials have been preliminarily selected and analyzed for the EFTV structure, namely: titanium alloy, copper, C/C-SiC and zirconia for surface coatings. This should give a first estimate of the characteristic behavior of potential materials specifically for this flight trajectory.

Titanium alloys exhibit a unique combination of mechanical and physical properties and corrosion resistance which have made them desirable for critical, demanding aerospace applications, also in high temperatures conditions. Copper is employed as a heat sink to accommodate the thermal energy in some critical components (e.g. nose, leading edges). C/C-SiC developed at DLR [11] and tested in different high temperatures applications (e.g. HIFiRE and SHEFEX) is considered for ailerons and for the final part of the wing leading edge. A zirconia coating layer has been also considered to protect titanium and copper components, increasing their surface emissivity and confining the larger temperatures on the layer itself.

Thermal and mechanical properties of titanium alloy and zirconia coating have been provided by TsAGI, Tsentralniy Aerogidrodinamicheskiy Institut (Central Aerohydrodynamic Institute), which is in charge of the system manufacturing.

In particular, the following assumptions, reported in Table 2, have been carried out on the vehicle components shown in Figure 7 to assess the correct implementation of the methodology:

- copper for the vehicle nose;
- copper for the fore part of the wing leading edges;
- C/C-SiC for the remaining part of the wing leading edge;
- copper for the leading edge of the V-tails;
- C/C-SiC for the ailerons;
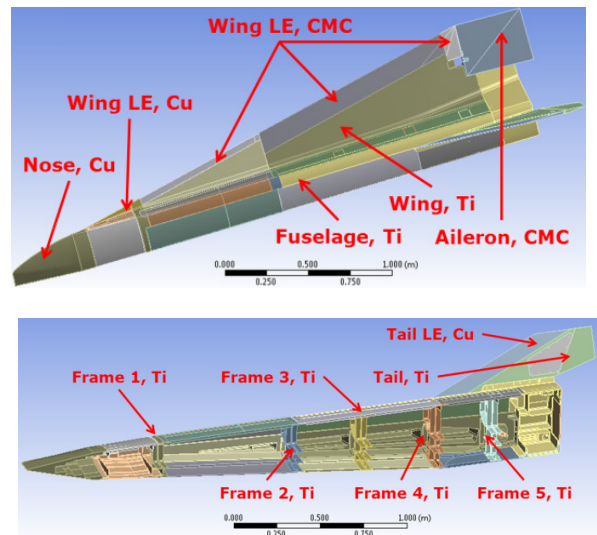- titanium alloy for the remaining part of the structure.

Figure 5. Main structural components of the analyzed EFTV

In addition, as previously mentioned, a layer of 1 mm thick zirconia has been foreseen for all the components in titanium alloy and copper. Using a conservative approach, a constant surface emissivity of 0.4 has been set for the external coated surfaces.

Table 2.Preliminarily material assignment for the main structural components

Nose	Fuselage	Wing
Copper	Ti-Alloy	Ti-Alloy
Wing LE	**V-Tail**	**Aileron**
C/C-SiC / Copper	Ti-Alloy / Copper	C/C-SiC

4. STRUCTURAL LAYOUT

The vehicle layout incorporates the contributions provided by the project partners for the following subsystems:

- Cold structure
- Hot structures
- Power System
- Inertial Platform and Flight Control System
- Telemetry and Tele-Command System
- In-Flight Measurement instrumentation

In this paper the cold and the hot structures layout are presented in more details.

4.1 COLD STRUCTURE

The cold structures of EFTV are composed mainly by the following major items:

- fuselage
- wings
- rudders

In particular, the fuselage structure will be realized with a build-up approach. Its structure is composed by three main sections:

- forward (FWD) fuselage
- central (CTR) fuselage
- tail fuselage

In Figure 6 the exploded view of the entire vehicle is reported. Figure 7 and Figure 8 show the main fuselage sections. In these figures is possible to identify all the components of the major items.
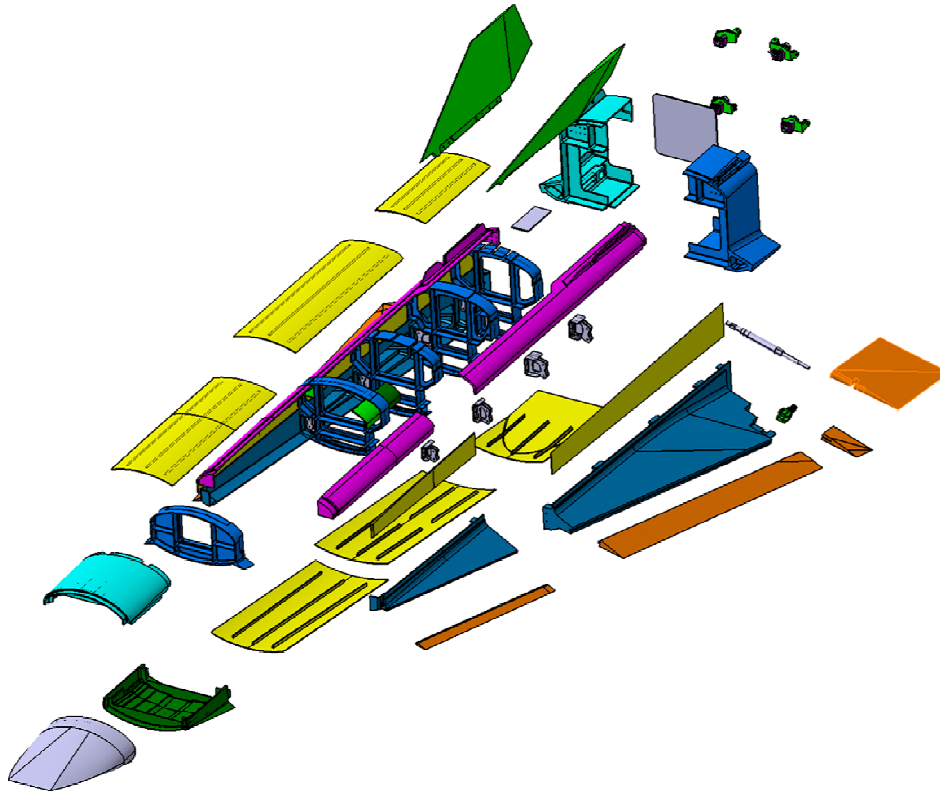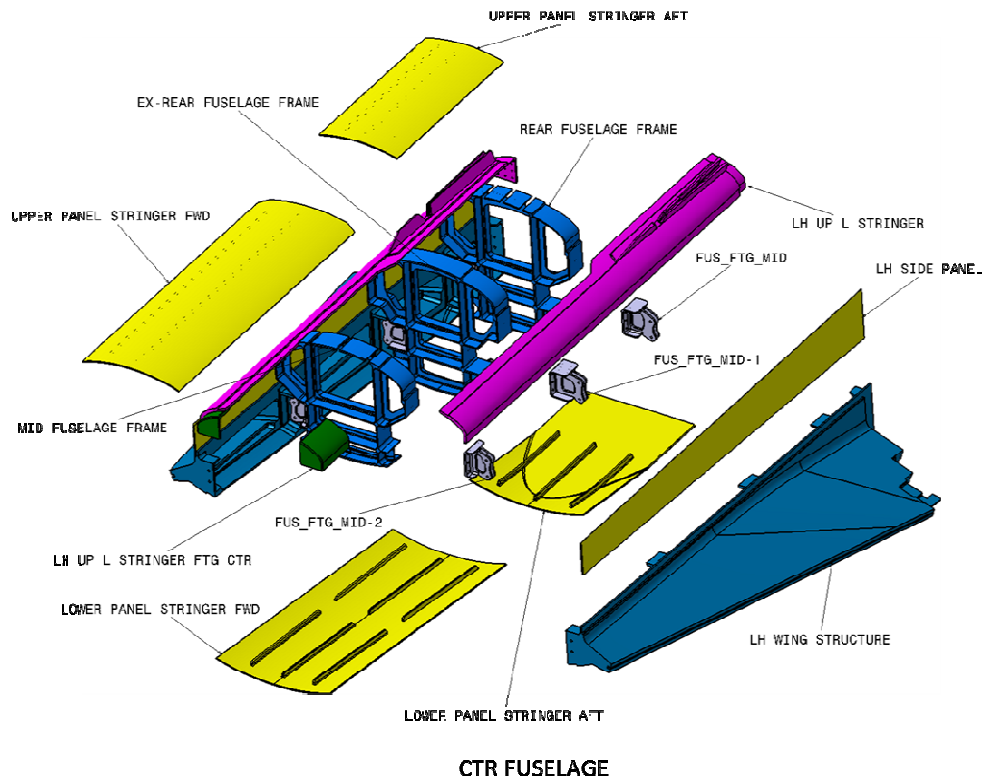

Figure 6.Main structural components

UPPER PANEL STRINGER AFT

EX-REAR FUSELAGE FRAME

REAR FUSELAGE FRAME

UPPER PANEL STRINGER FWD

LH UP L STRINGER

FUS_FTG_MID

LH SIDE PANEL

FUS_FTG_MID-1

MID FUSELAGE FRAME

FUS_FTG_MID-2

LH UP L STRINGER FTG CTR

LOWER PANEL STRINGER FWD

LH WING STRUCTURE

LOWER PANEL STRINGER AFT

CTR FUSELAGE

Figure 7. CTR fuselage main structural components

UPPER PANEL NOSE

FWD FUSELAGE FRAME FROM MID

TAIL SOLID-RH

TAIL SOLID PANEL

LH UPP L NOSE STRINGER FTG

LH NOSE PANEL

FUS_FTG_FWD

TAIL SOLID

FWD FUSELAGE FRAME

TAIL SOLID STRAP

LH NOSE STRINGER LWR

LH UPP L NOSE STRINGER

LOWER PANEL NOSE

TAIL FUSELAGE
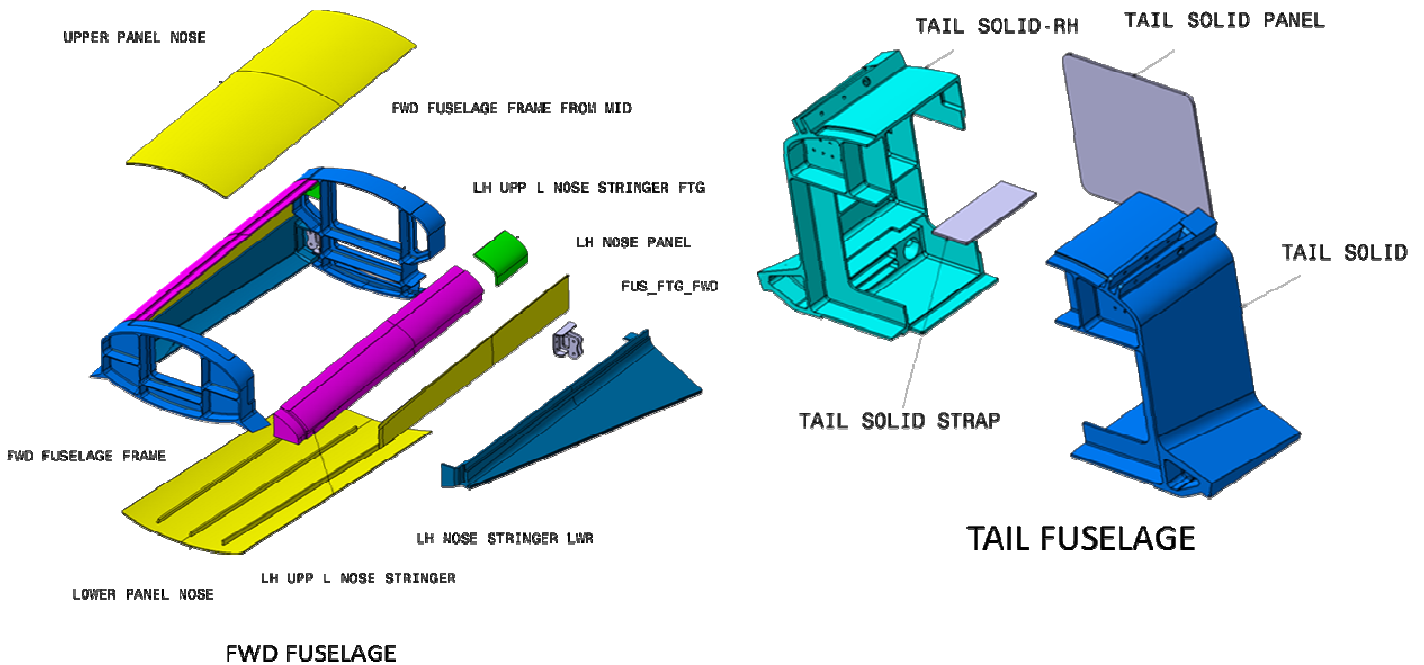
FWD FUSELAGE

Figure 8. FWD and Tail fuselage main structural components

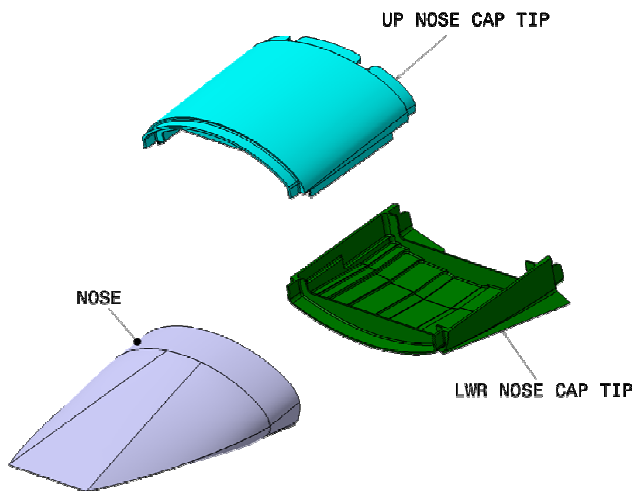*Figure 9. Nosecap structural components*

Figure 10. Leading edge and aileron structural components

4.2 HOT STRUCTURE

The hot structures of EFTV are composed mainly by the following subsystems:

- ailerons
- wing Leading edge
- nose cap

The nose is composed by three parts, one fully solid body in copper and two shells (upper and lower shell), designed in titanium alloy and longitudinally joint one to each other.

For a first approach, the first part of the nose is designed as one fully solid body which can be manufactured as integral part. Considering the large heat fluxes expected on the vehicle nose, copper is chosen for its ability to work as a heat sink. The two shells are manufactured by milling tools, starting from a titanium plate. The junctions will be done by bolts. In Figure 9 the exploded view of nose cap is shown.

Figure 10 reports the aileron and the wing leading edges colored in orange. These components will be made of the C/C-SiC developed at DLR [11].

5. THERMAL ANALYSIS

5.1 NUMERICAL PROCEDURE

The vehicle thermal behavior has been preliminary assessed by means of the Finite Element Method (FEM) implemented in the software Ansys [12-13]. A transient analysis along the computed entry path is performed to evaluate the time dependent temperature of the structure. In synthesis, as also schematically reported in Figure 11, the following procedure has been carried out:
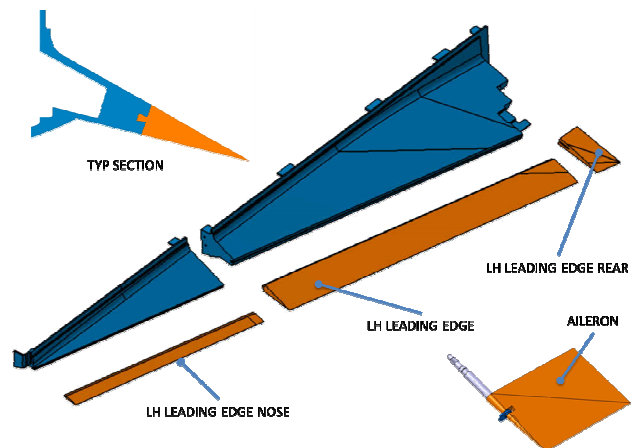
- the available CAD drawing of the vehicle is implemented in Ansys Workbench and properly modified, if required;
- the computational mesh for the subsequent analyses is generated;
- the transient thermal analysis is set assuming as boundary condition the convective heat transfer coefficient spatial distribution over the vehicle surface, evaluated in a certain number of flight conditions by means of stationary CFD calculations. These distributions are properly scaled by the stagnation-point heat transfer coefficient variation along the trajectory, normalized with respect to the corresponding reference condition (see Figure 11). A radiative dissipation condition is also considered for all the external surfaces;
- static structural computations can be then carried out, if required, in the most critical conditions along the trajectory, assigning as boundary conditions the temperature distributions previously evaluated at selected instants along the trajectory and the pressure distribution resulting from CFD analyses.

As previously mentioned, the boundary condition for the transient thermal analysis has been assigned in terms of the convective heat transfer coefficient, so that the FE numerical code can take into account the effective heat flux entering the structure as the wall temperature increases under the heating process. The stagnation-point convective heat transfer coefficient variation over the trajectory has been obtained from the corresponding convective heat flux profile, estimated by means of the Tauber's [10] relationship throughout the descent flight (see Equation 1, valid assuming an ideal gas condition and a constant specific heat).
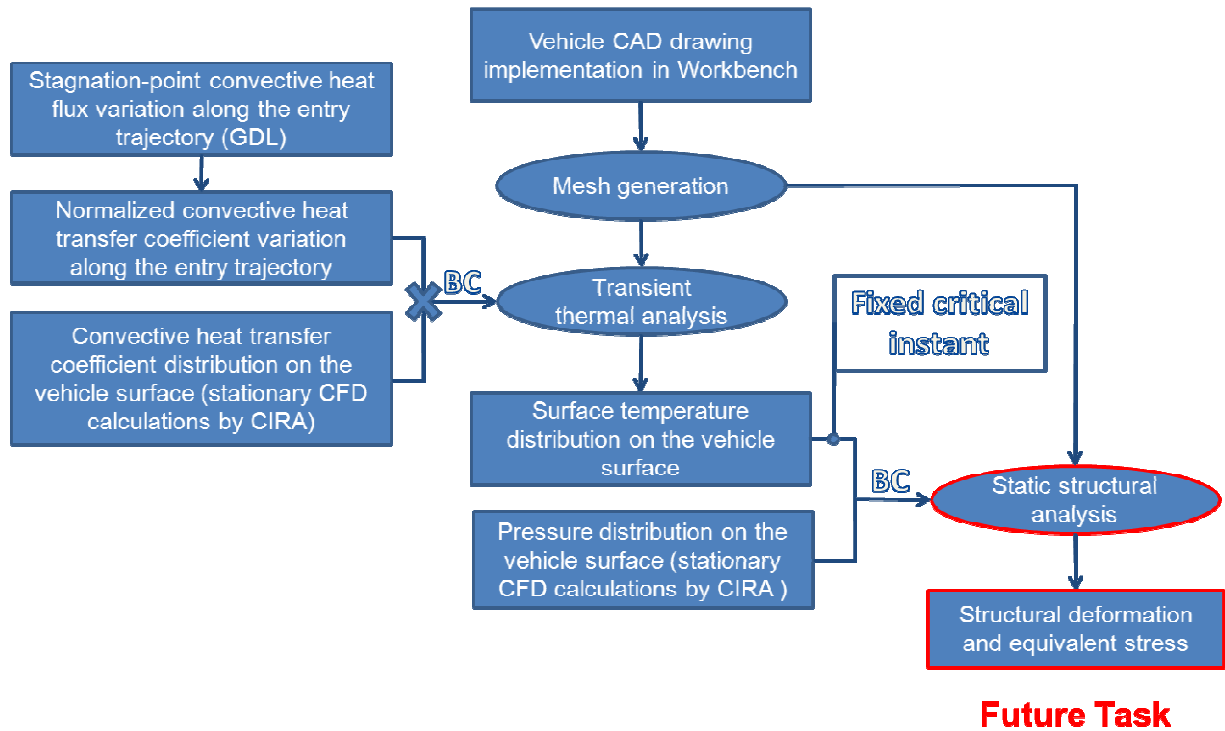
Figure 11. Numerical procedure flow chart

$$\dot{q} = h \cdot \left(T_0 - T_w\right) \approx \frac{\dot{q}_{cw}}{T_{aw}} \cdot \left(T_{aw} - T_w\right) =$$

$$= \frac{\dot{q}_{hw,eq}}{T_{aw} - T_{w,eq}} \cdot \left(T_{aw} - T_w\right) \qquad (1)$$

It is clear that the convective heat transfer coefficient at any point of the vehicle surface and at a certain time instant can be obtained multiplying the value of the heat transfer coefficient at the selected spatial point (resulting from the CFD calculation), by the normalized stagnation-point convective heat transfer coefficient along the flight path at the selected time instant.

5.2 PRELIMINARY RESULTS

As results, according to the previously discussed method, the temporal variation of the maximum temperature on the different analysed materials and vehicle components has been plotted along the flight path. Figure 12 reports in particular the maximum temperature variation along the flight profile on the main vehicle components.

From Figure 12 it can be seen that zirconia coatings and C/C-SiC components (having maximum service temperatures in the order of 2400°C and 1600°C, respectively) would widely survive the aerothermal environment in these conditions. On the other hand, it can be noted that the maximum temperatures on the titanium and copper structures slightly exceed their upper working temperature limits (600 and 800°C, respectively), but only in limited spots of the vehicle, coloured in red for the titanium structure in Figure 13. This means that such temperature overshoot can be in principle redistributed inside the vehicle structure through a future thermal structural optimization.
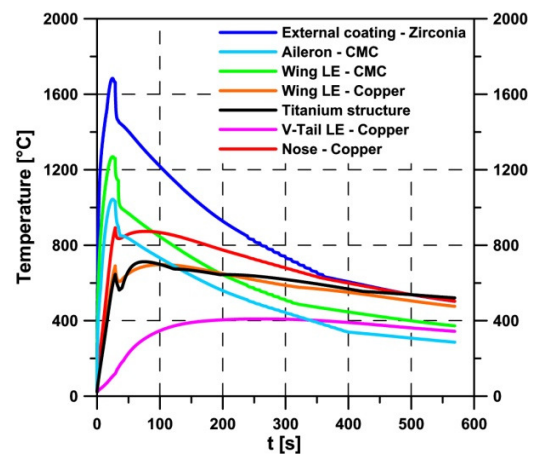

Figure 12. Maximum temperature along the flight profile on the main vehicle components
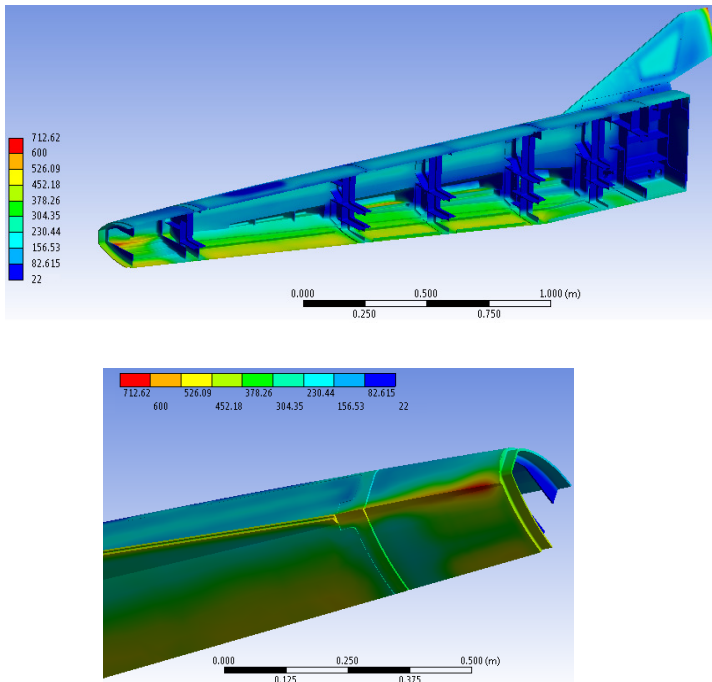
Figure 13. Temperature distribution, at the peak heating condition for titanium components

6. CONCLUSIONS

Finally, it can be concluded that:

- a thermal model has been realized for the entire structure on the basis of aero-thermal loads estimated along the flight path;
- zirconia coating guarantees a relatively large surface emissivity and a suitable thermal protection for the underlying materials;
- copper seems to be adequate for the nose and the first part of the wing leading edge, considering its ability to work as a heat sink;
- copper and titanium structures can withstand the aerothermal environment except for limited spots, requiring a proper thermal structural optimization;
- thermal structural design is still ongoing and a numerical analysis campaign will be perform on updated structural configuration, flight trajectory and aerothermal environment.

ACKNOWLEDGMENTS

REFERENCES

1. Steelant J. (2009). Achievements obtained on Aero-Thermal Loaded Materials for High-Speed Atmospheric Vehicles within ATLLAS. In Proc. 16th AIAA/DLR/DGLR "International Space Planes and Hypersonic Systems and Technologies Conference", Bremen, Germany, AIAA-2009-7225.

2. Steelant, J. (2011). Sustained Hypersonic Flight in Europe: first achievements within LAPCAT II. In Proc. 17th AIAA "International Space Planes and Hypersonic Systems and technologies conference", San Francisco, California, AIAA 2011-2243.

3. Steelant, J. et al. (2015). Conceptual Design of the High-Speed Propelled Experimental Flight Test Vehicle HEXAFLY. In Proc. 20th AIAA "International Space Planes and Hypersonic Systems and technologies conference", Glasgow, Scotland, AIAA 2015-3539.

4. Hexafly-INT Team (2014). Part B "High-Speed Experimental Fly Vehicles–INTernational", CIRA-CF-14-1132

5. Jung, W., Ettl, J., Kallenbach, A., Turner, J. (2014). Mission Definition and System Requirements, Work Package 2.0 – Launch Vehicle, Presentation at HEXAFLY-INT MDR & SRR, Capua, Italy

6. Favaloro, N., Rispoli, A., Vecchione, L., Pezzella, G., Carandente, V., Scigliano, R., Cicala, M., Morani, G., Steelant, J. (2015). Design Analysis of the High-Speed Experimental Flight Test Vehicle HEXAFLY-International. In Proc. 20th AIAA "International Space Planes and Hypersonic Systems and technologies conference", Glasgow, Scotland, AIAA 2015-3607

7. Pezzella, G., Marini, M., Reimann B., Steelant, J. (2015). Aerodynamic Design Analysis of the HEXAFLY-INT Hypersonic Glider. In Proc. 20th AIAA "International Space Planes and Hypersonic Systems and technologies conference", Glasgow, Scotland, AIAA 2015-3644

8. Pezzella, G., van Brummen, S., Steelant, J. (2015). Assessment of Hypersonic Aerodynamic Performance of the EFTV-ESM Configuration in the Framework of the Hexafly-INT Research Project. In Proc. 8th European Symposium on Aerothermodynamics for Space Vehicles, Lisbon, Portugal

9. Pezzella, G., Carandente, V., Scigliano, R., Marini, M., Steelant J. (2015). Aerothermal Environment Methodology of the Hexafly-INT Experimental Flight Test Vehicle (EFTV). In Proc. 8th European Symposium on Aerothermodynamics for Space Vehicles, Lisbon, Portugal

10. Tauber, M.E. (1989). A review of high-speed, convective, heat-transfer computation methods. Technical Paper 2914, NASA.

11. Glass, D.E., Capriotti, D.P., Reimer, T., Kütemeyer, M., Smart, M. (2014). Testing of DLR C/C-SiC and C/C for HIFiRE 8 Scramjet Combustor. In Proc- 19th AIAA "International Space Planes and Hypersonic Systems and Technologies Conference", Atlanta, Georgia

12. ANSYS Inc. (2009). Thermal analysis guide, Release 12.1.

13. ANSYS Inc. (2009). Structural analysis guide, Release 12.1.